

CTF3 photo-injector laser system: Conversion to UV

M. Petrarca¹, V. Fedosseev¹, N. Lebas¹
G. Cheymol²

1) CERN, Geneva, Switzerland

2) CEA, Saclay, France

Abstract

In this note, the implementation on the CTF3 photo-injector laser chain in order to perform harmonic generation is explained. The conversion efficiency measurements for the second, IR to Green, and fourth, Green to UV, harmonic generation are described.

1. Introduction

The CTF3 photo-injector laser system has been designed and constructed by RAL. The material was transferred to CERN in September 2006. The setting up and testing of the laser system is on-going, in collaboration between INFN Frascati, University of Milano and CERN. In parallel with the PHIN photo-injector (intended as CTF3 drive beam source), a fraction of the laser pulses can be used for the CALIFES probe beam at CTF3. This work is being done in collaboration between CEA and CERN.

2. The CTF3 photo-injector laser system

The photo-injector laser system designed for the CTF3 drive beam is described below. A schematic layout is given in Figure 1.

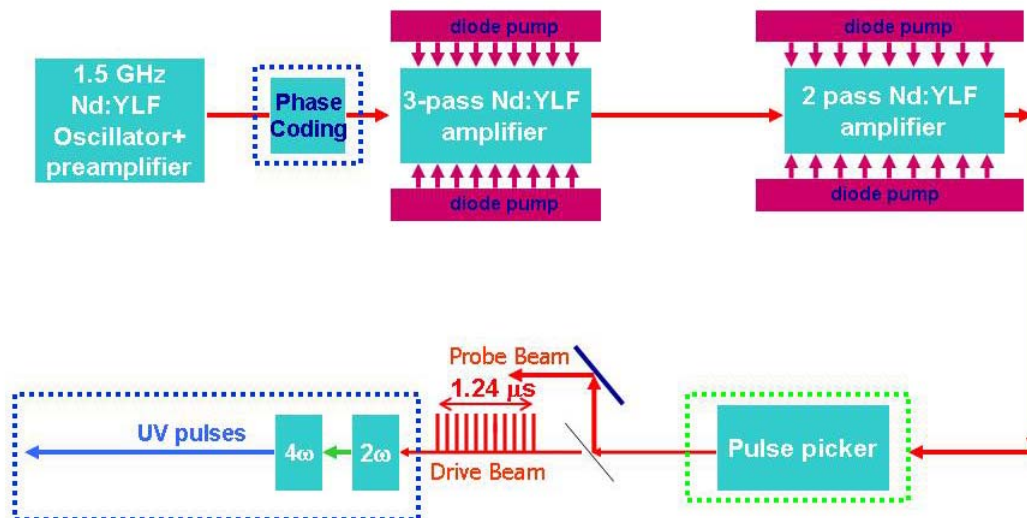


Figure 1: CTF3 photo-injector laser system

A Nd:YLF oscillator¹ produces vertically polarized pulses at a repetition rate of 1.5GHz (~ 666 ps between two consecutive pulses) with an average power of $P \sim 300$ mW, a central wavelength $\lambda \sim 1047$ nm and with a pulse time width of $\tau \sim 6$ ps. These pulses are first amplified by a Nd:YLF “pre-amplifier”² required to increase the average power up to $P \sim 10$ W. The pulses delivered by the pre-amplifier have the same characteristics ($\tau \sim 6$ ps (FWHM) and $\lambda \sim 1047$ nm). In between the oscillator and the preamplifier a dedicated device called “Phase Coding” will be placed. This equipment provides a special time distribution of the pulses necessary to produce electron bunches with a distribution in time as required for the CTF3 delay loop

After these first stages, the laser beam is injected sequentially into two powerful Nd:YLF amplifiers: the first one is made up of a $L_1 = 8$ cm long Nd:YLF rod with $d_1 = 7$ mm diameter

¹ High Q Laser Production GmbH model *picoTRAIN* IC-1047-10000-ps Nd:YLF 1.5GHz Sync

² High Q Laser Production GmbH model *picoTRAIN*

aperture pumped by 5 stacks of diode lasers symmetrically arranged around the rod. The total diode pump peak power is 15 kW and its amplification window is $\tau_1 \sim 400 \mu\text{s}$. The second amplifier has a rod length $L_2 = 12 \text{ cm}$ and diameter $d_2 = 10 \text{ mm}$; it is diode-pumped by 5 diode arrays symmetrically arranged around the rod, the pumping peak power is 17 kW and its amplification window is $\tau_2 \sim 200 \mu\text{s}$. This amplification starts with a delay of $200 \mu\text{s}$ with respect to the starting time of the first amplifier. In some measurements a longer amplification window ($\tau_2 \sim 250 \mu\text{s}$) was applied with correspondingly decreased delay between the first and second amplifiers.

Both amplifiers are designed to work at a repetition rate in the range of 5 –50 Hz.

After the second amplifier, a Pockels cell allows to select the pulse train length, according to the requirements of the CTF3 RF gun. Ultimately, the CTF3 drive beam will require a $1.272 \mu\text{s}$ long train of pulses at 1.5 GHz, with a repetition rate of up to 50 Hz. Presently, a repetition rate of 5 Hz is being used.

Further details concerning the laser system are given in references [1] and [2].

3. Set up for the conversion process

In order to test the conversion efficiency process, the set-up shown schematically in Fig 2 and in more detail in Fig 3, has been used. The second amplifier is off; the first amplifier has been used for three main different drive diode currents of 65, 75 and 85 A. The macro-pulse from the first amplifier is sent into the pulse picker (Pockels cell system) by which a $2 \mu\text{s}$ slice in the saturation region of the macro-pulse is cut. This beam is first sent into a lens system (shown in Fig. 3) needed to control the beam waist dimension on the non-linear crystal. After this, the beam is sent into the Second Harmonic (SH, 2ω) and Fourth Harmonic (FH, 4ω) crystals. Between the two crystals a lens system (L1a and L1b, see Fig. 3.) is placed in order to do an imaging of a plane located in the SH crystal into the FH crystal in order to keep a good focusing in the two crystals. Note that the lenses system introduces a zoom factor of 1.2, which can presently not be avoided due to lack of appropriate lenses.

For the SH process an 10 mm thick KTP_H crystal (KTiOPO_4 Potassium titanyl phosphate, hydrothermally grown) has been used to perform a Type II interaction process ($1047|e\rangle + 1047|o\rangle = 523|e\rangle$) where $|o\rangle$ and $|e\rangle$ indicate respectively the ordinary and extraordinary state of polarization). The KTP_H crystal has been chosen because of its high value for the “effective non-linear coefficient” $d_{\text{eff}} \sim 3.16 \text{ pm/V}$ which leads to the highest conversion efficiency.

For the FH process a 12 mm thick BBO (beta barium borate) frequency doubling crystal has been chosen to perform a Type I interaction process ($523|o\rangle + 523|o\rangle = 262|e\rangle$), its nonlinear effective coefficient is $d_{\text{eff}} \sim 1.73 \text{ pm/V}$.

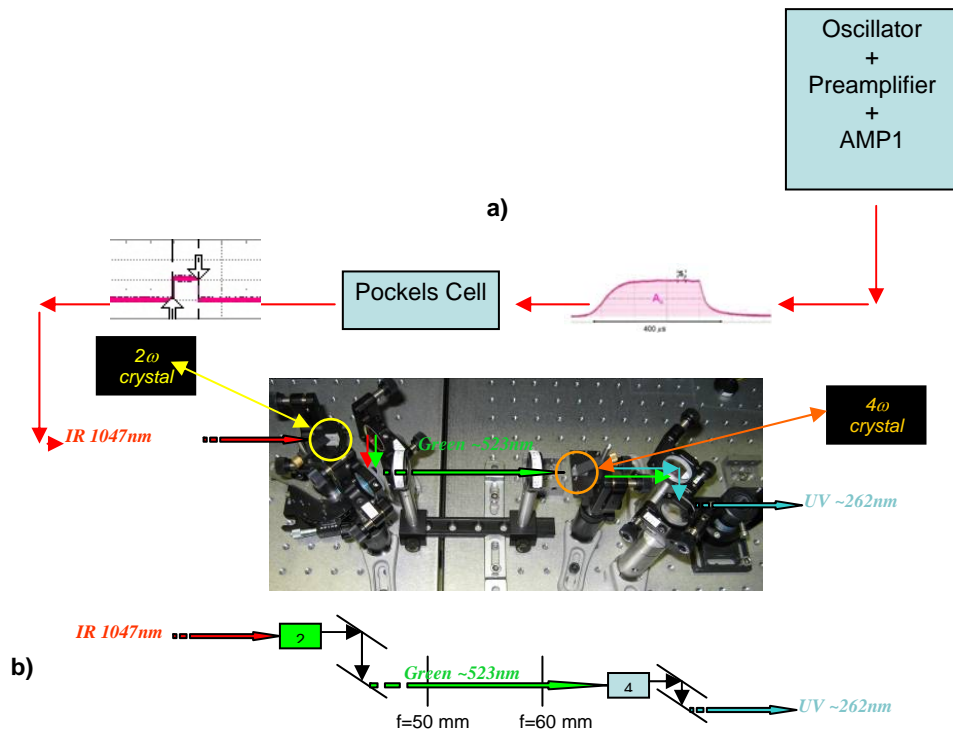


Figure 2: **a)** A 2 μ s slice of the the macro-pulse beam coming from the first amplifier is sent into the second harmonic crystal and then into the fourth harmonic one in order to convert IR (1047nm) light into Green (523) and then into UV (262nm). **b)** Schematic layout of the same crystal disposition shown (zoomed) on the photograph above.

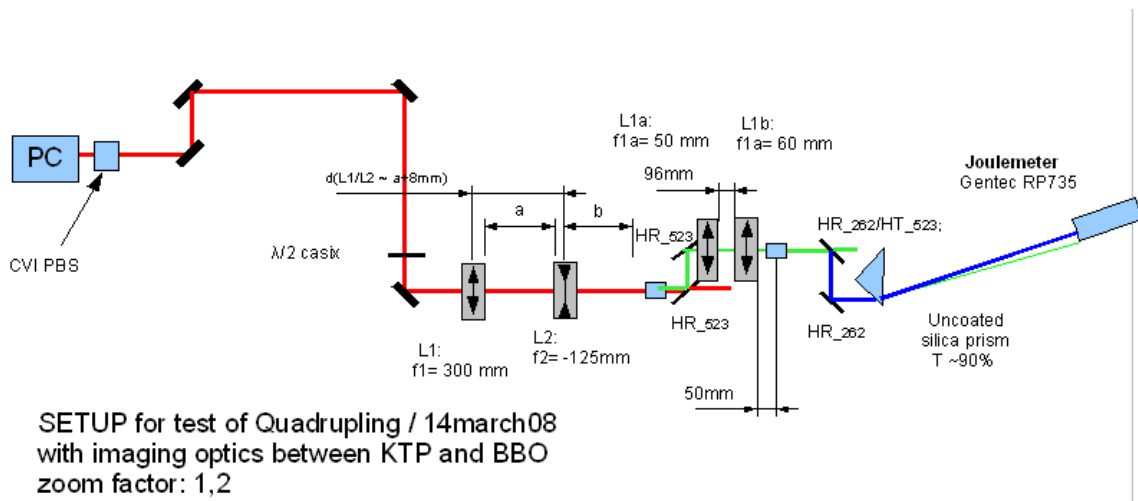


Figure 3: The complete optical layout for the harmonic conversion process is shown. The IR laser beam coming from the pulse picker (Pockels Cell + PBS) is sent into the L1 and L2 lenses system needed to control the beam waist dimension on the SH crystal. After the SH crystal the lens system composed by L1a and L1b, images the middle plane of the first crystal onto the second one introducing a magnification on 1.2. Following the FH crystal there are two high reflection mirrors for UV and a prism which are used to definitely spatially separate the UV Green from the IR beam. Finally the UV beam is sent into the joule meter.

4. Second and Fourth harmonic conversion tests

A number of tests have been performed to convert the 2 μ s slice of the IR (1047 nm) amplified beam, which has been selected by the Pulse Picker at the exit of the second amplifier, to green light (523 nm). Measurements have been performed to find a configuration which gives the highest conversion efficiency when the first amplifier is running at full power. No one of those measurements gave a satisfactory result. Even when the beam size onto the crystal was strongly reduced (115 μ m) a very low conversion efficiency of 10% has been reached, for such a critical configuration in which the crystal coating started being damaged because of the high power density.

The low conversion efficiency led us to consider the time structure of the amplified laser beam. Investigations of the amplified beam using a fast detector from “New Focus” coupled to a digitizing scope revealed that the first amplifier should be used only at 65 A diode driving current (nominal power uses 90 A current in the diodes) otherwise most of the laser beam energy is found outside the micro-pulses structure at 1.5GHz.

With this driving current (65A), several other conversion efficiency measurements have been performed. The highest value for the conversion efficiency from IR to green has been measured to be ~44% for a 200 μ m FWHM beam size onto the SH crystal. This beam size seems to be reasonable since we are far from the limits of damaging the crystal coating - thus we decided to adopt this waist size on the crystal for all further measurements.

A set of conversion efficiency measurements has also been taken when the pumping driving diode current was increased from 65 to 75 and 85 A (a condition in which the photo-detector measurements clearly shows a non satisfactory time structure, indicating that the laser energy is not concentrated in the micro-pulses). The beam spot size has been adjusted for each measurement. We took special care to place the crystal always on the waist of the beam whose size has been kept fix to about 200 μ m FWHM (see Fig 4). The experimental results, shown in Table 1, demonstrate that with the actual configuration of the first amplifier, the best conversion efficiency value of 44% can be achieved for 65A driving current; by increasing the driving current the conversion efficiency drops to unacceptable values³.

This is in agreement with the unsatisfactory time structure observed with the photodetector at those drive diode current values.

Diode driving current [A]	IR energy \pm Std [mJ]	Green energy \pm Std [mJ]	SHG efficiency (1047 \rightarrow 523)nm
65	1.30 \pm 0.03	0.57 \pm 0.14	44%
75	1.75 \pm 0.04	0.50 \pm 0.14	29%
85	2.43 \pm 0.08	0.31 \pm 0.23	13%

Table 1: The conversion efficiency values (column 4) are reported for different driving current values of the pumping diode (column 1). The IR energy of the 2 μ s slice of the amplified beam is reported (column 2) as well as the green energy (column 3) coming from the conversion.

³ It should be mentioned that the absolute value of available energy in IR is much below specification - improvements on the amplifier chain are necessary to remedy this problem.

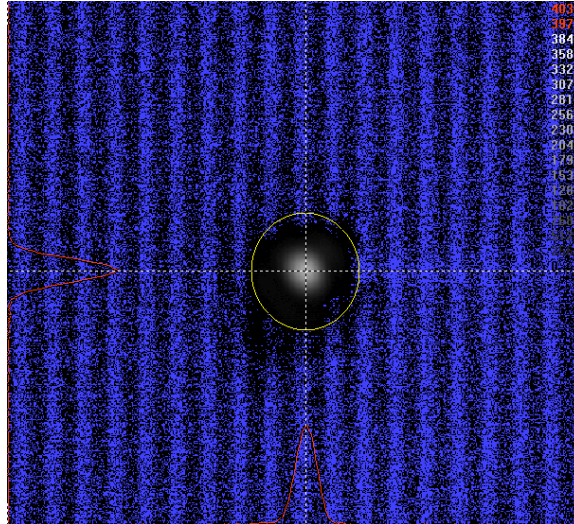


Figure 4: IR beam waist on a plane where the SH middle crystal point has been placed for the first amplifier running at 65A, X=186 μm (StdX=4.2 μm), Y=205um (StdY=7,1 μm)

To perform the conversion from green light to UV, a lens system (L1a and L1b in Fig. 3) has been placed between the KTP and the BBO crystals as described above. For the first amplifier running at 65 A the highest conversion efficiency $\sim 22\%$ has been reached yielding a UV micro pulse energy of ~ 40 nJ.

By increasing the driving current for the first amplifier the conversion efficiency to UV again drops down to unsatisfactory values. The reason for this behavior is the same as for the SH conversion process.

The UV transverse profile is shown in Figure. 5. The elongated shape is mainly due to the spatial walk-off angle introduced by the BBO: $\alpha_{\text{max}} = 80$ mrad for the extraordinary ray; such walk-off angle for a crystal length of $L=12$ mm will give about $L \cdot \alpha_{\text{max}} = 1$ mm spatial separation (spatial walk-off) in the output of the crystal; this separation is also more visible in our configuration in which the beam waist dimension onto the crystal is very small $\sim 200\mu\text{m}$.

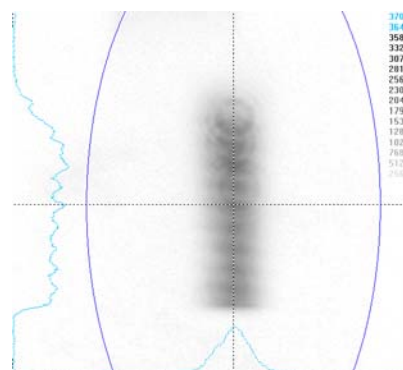


Figure 5: Image of the UV beam waist in the output of the BBO crystal. The elongated shape is due the walk-off angle introduced by the BBO crystal and it is in agreement with the measured dimension $\sim 1000 \mu\text{m}$ for and input waist of $\sim 200\mu\text{m}$ ($\alpha_{\text{max}} \cdot L \sim 1\text{mm}$).

5. Summary

The crystals for the second and fourth harmonic conversion process have been installed along the CTF3 photo-injector laser chain in order to convert sequentially the IR (1047nm) to Green (523nm) and then to UV (262nm).

Several schemes has been tested to achieve a high efficiency second harmonic generation; a satisfactory result, ~44% of efficiency, has been achieved for a 200 μm FWHM beam waist on the KTP_H crystal with the first amplifier running at 65A. In this configuration, a lens system to image the IR beam waist on the second harmonic crystal to the fourth harmonic one has been introduced and the highest measured conversion efficiency was ~22%. The highest UV micro-pulse energy achieved was ~ 40nJ.

The conversion measurements performed so far revealed that the first amplifier is not working properly, yielding a lot of energy outside the micro-pulse for diode drive currents above 65A. Further work is thus necessary to investigate the behavior of the first amplifier and improve its performance.

References

- 1) M. Divall et al., "Design and testing of amplifiers for the CTF3 photo-injector laser", CARE-Report-06-021-PHIN
- 2) M. Petrarca et al., "CTF3 photo-injector amplifiers construction", CARE-Report-2008-012-PHIN